

Drug Bioconjugates

International Edition: DOI: 10.1002/anie.201602702
German Edition: DOI: 10.1002/ange.201602702

N-Heterocyclic Carbene–Gold(I) Complexes Conjugated to a Leukemia-Specific DNA Aptamer for Targeted Drug Delivery

Weijia Niu⁺, Xigao Chen⁺, Weihong Tan, and Adam S. Veige*

Abstract: This report describes the synthesis and characterization of novel N-heterocyclic carbene (NHC)–gold(I) complexes and their bioconjugation to the CCRF-CEM-leukemia-specific aptamer sgc8c. Successful bioconjugation was confirmed by the use of fluorescent tags on both the NHC–Au^I complex and the aptamer. Cell-viability assays indicated that the NHC–Au^I–aptamer conjugate was more cytotoxic than the NHC–gold complex alone. A combination of flow cytometry, confocal microscopy, and cell-viability assays provided clear evidence that the NHC–Au^I–aptamer conjugate was selective for targeted CCRF-CEM leukemia cells.

N-Heterocyclic carbenes (NHCs) are an interesting class of ligands with strong σ -donating properties.^[1] The resulting strong bond between transition metals and NHCs renders their metal complexes stable to air, heat, water, and acid.^[2] In the context of potentially reducing the side effects caused by metallodrug demetalation and degradation in the body, NHC–metal complexes offer a promising alternative, especially considering their ease of synthesis and vast structural diversity.^[3,4] In the last decade, NHC–Au complexes have drawn attention as a new generation of potential anticancer agents owing to their impressively high cytotoxicity and stability. A series of neutral and cationic NHC–Au complexes with a wide diversity of ligand structures have been synthesized and characterized.^[3–5] NHC–Au^I complexes can induce cell apoptosis by targeting mitochondrial-related cellular pathways^[6,7] that involve thioredoxin reductase (TrxR) and estrogen receptor (ER).^[3,7] Although NHC–Au^I complexes inhibit the growth of tumor cells, they also interact with normal human cells, a characteristic common to metal-based drugs,^[8] thus limiting their potential as cancer therapeutics.^[9,10] Cell selectivity is an area clearly in need of improvement.

We now describe a strategy to target cancer cells efficiently while potentially reducing metal-related side effects. The strategy involves the covalent binding of a cytotoxic NHC–Au^I complex to a DNA aptamer. Aptamers are short single-stranded oligonucleotides that are biocompatible, stable, and more importantly, able to specifically recognize

and effectively bind to their targets, in this case cancer cells.^[11] With all these advantages, DNA aptamers are among the most attractive drug-delivery agents.^[12–14] Several reported studies have featured aptamer–drug conjugates, but most rely on the noncovalent association of the drug with specific DNA sequences.^[13] Noncovalent strategies have disadvantages, such as complicated syntheses, uncontrollable drug loading, and uncontrollable drug release.^[15] One study on covalent attachment involved tethering of the anticancer agent doxorubicin (Dox) to an aptamer.^[14] However, Dox causes side effects, such as congestive heart failure^[16] and typhlitis.^[17] Furthermore, resistance to Dox is common, which represents a major obstacle to successful treatment.^[18]

Herein, we describe the bioconjugation of a NHC–Au^I complex to an aptamer (Figure 1) and demonstrate its cancer-cell-specific internalization and cytotoxicity. The sgc8c aptamer was chosen as the model drug carrier. The sgc8c aptamer is able to recognize and target, with high binding affinity, the protein tyrosine kinase 7 (PTK-7), a transmembrane receptor protein highly expressed on CCRF-CEM leukemia cells.^[19] The formation, selectivity, and cytotoxicity of the aptamer–drug conjugates were verified by fluorescence spectroscopy, high-performance liquid chromatography, flow cytometric analysis, confocal fluorescence microscopy, and MTS cell-proliferation assays (MTS = 3-(4,5-dimethylthiazol-2-yl)-5-(3-carboxymethoxyphenyl)-2(4-sulfophenyl)-2H-tetrazolium).

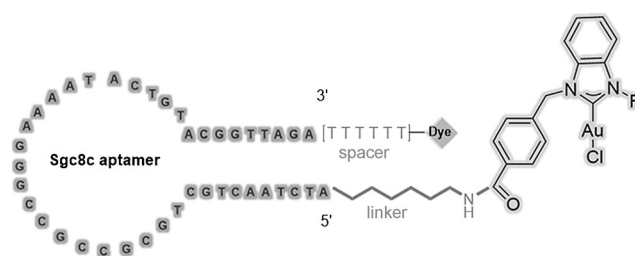


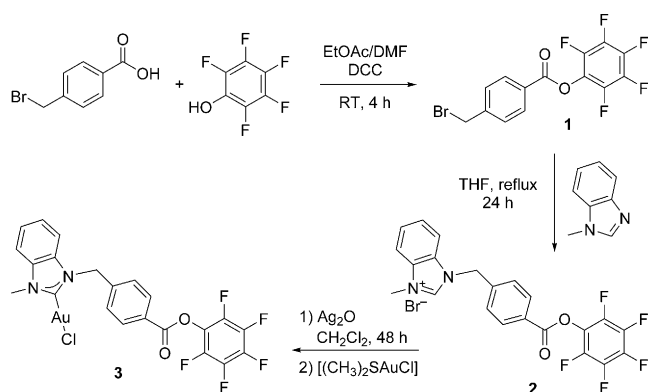
Figure 1. Design of the aptamer–NHC–Au^I conjugate.

The half-life of an amide bond is approximately 600 years in solution at pH 7 and ambient temperature.^[20] The stability and biocompatibility of amide linkages make them highly attractive for site-specific bioconjugation.^[21] As compared to alkyl esters, activated esters, such as pentafluorophenyl esters (Pfp esters), react with a wider range of nucleophiles.^[22] More importantly, activated esters are stable in the solid state but react rapidly with amines in solution under mild conditions to give the desired amides in high yield and with high purity.^[23,24] Therefore, our synthetic design involves functionalizing

[*] W. Niu,^[+] X. Chen,^[+] W. Tan, A. S. Veige
University of Florida, Department of Chemistry
P.O. Box 117200, Gainesville, FL (USA)
E-mail: veige@chem.ufl.edu
Homepage: <https://veige.chem.ufl.edu/>

[+] These authors contributed equally to this work.

Supporting information and the ORCID identification number(s) for the author(s) of this article can be found under <http://dx.doi.org/10.1002/anie.201602702>.



Scheme 1. Synthesis of the Pfp-ester-functionalized NHC–Au^I complex **3**. DCC = *N,N'*-dicyclohexylcarbodiimide, DMF = *N,N*-dimethylformamide.

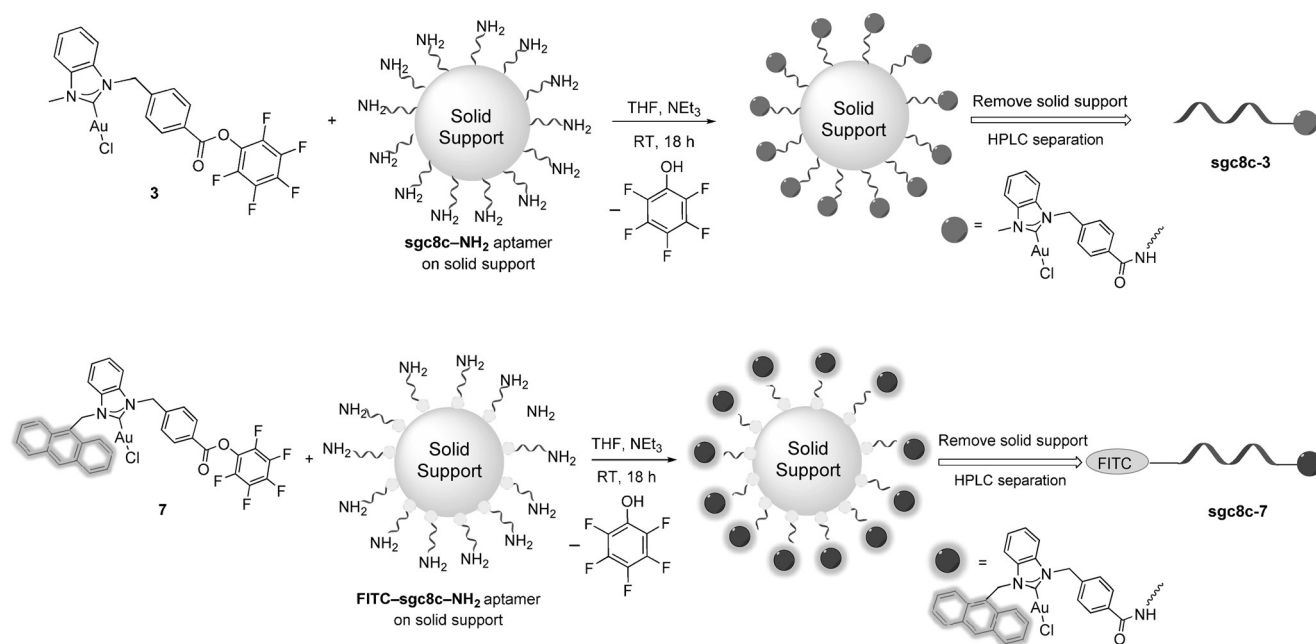
a NHC ligand with a Pfp-ester group (Scheme 1), metalation with Au^I, and subsequent bioconjugation to an amine group at the 5' end of the DNA aptamer sgc8c.^[25]

A two-step procedure yielded the benzimidazolium NHC–Pfp ligand precursor **2** (Scheme 1).^[23] As confirmation of its identity, the ¹H NMR spectrum of **2** exhibited a typical downfield resonance for the imidazolium C2 proton at 11.74 ppm. A notable signal in the ¹³C{¹H} NMR spectrum is the carbonyl resonance at 166.4 ppm. Silver(I) transmetalation with dimethylsulfidegold(I) chloride ((CH₃)₂SAuCl) provided the NHC–Au^I complex **3**. The downfield proton resonance observed for ligand **2** at 11.74 ppm was absent in the spectrum of complex **3**. In the ¹³C{¹H} NMR spectrum of **3**, the imidazole carbon resonance was shifted downfield from 141.3 ppm for **2** to 174.1 ppm. The carbonyl carbon resonance maintained its position at 166.8 ppm, thus suggesting the ester oxygen atoms do not interact with the Au^I ion. Finally,

resonances at 152.41, 157.72, and 162.16 ppm in the ¹⁹F NMR spectrum confirmed that complex **3** retained the Pfp-ester moiety. By employing an MTS cell-proliferation assay against the human T-lymphoblastic leukemia cell line CCRF-CEM, the cytotoxicity of complex **3** was evaluated (see the Supporting Information). With an IC₅₀ value of (14.6 ± 1.40) μM, complex **3** was found to be cytotoxic towards the target cell.

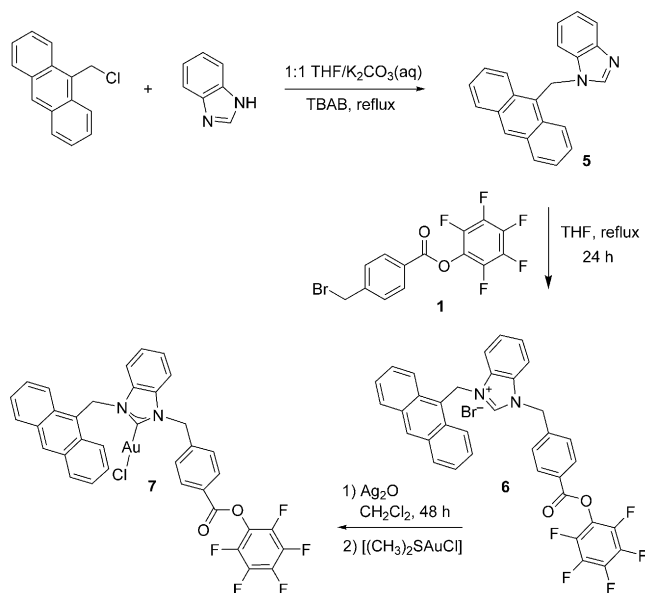
We next needed to develop a method to conjugate complex **3** to an amine-functionalized aptamer. Furfurylamine was used to mimic the amine-functionalized aptamer in a test reaction. The treatment of complex **3** with furfurylamine provided the NHC–Au^I–amide complex **4** in 91 % yield within 6 h (see the Supporting Information). After this successful test reaction, the NH₂-modified sgc8c aptamer was synthesized.^[26,27] For the bioconjugation reaction, the solid-supported aptamer (0.1 μmol, 1 equiv) was suspended in THF (500 μL) and treated with complex **3** (10 μmol, 100 equiv), followed by the slow addition of Et₃N (1.4 μL; Scheme 2). The mixture was shaken at ambient temperature for 18 h, and then the solid support was removed, and the resulting NHC–Au^I–aptamer conjugate **sgc8c-3** was purified by separation using HPLC (Scheme 2). An MTS assay of the aptamer–drug conjugate revealed an impressive increase in cytotoxicity as compared to that of complex **3** alone. The IC₅₀ value decreased from (14.6 ± 1.40) for **3** to (0.54 ± 0.85) μM. Possible explanations for the increased cytotoxicity include high affinity of the aptamer conjugate for the target cells and its efficient internalization into the cells, and the enhanced hydrophilic nature of the drug after conjugation to the aptamer.^[14,28]

As a tool for monitoring the fate of the aptamer and the NHC–Au conjugate independently, we constructed a dual-tagged aptamer–NHC–Au conjugate. The anthracenyl tag was chosen as a fluorescent signaling agent for the NHC–Au^I



Scheme 2. Strategy for the synthesis of aptamer–NHC–Au conjugates **sgc8c-3** and **sgc8c-7**.

fragment.^[29] Ligand **6** and the NHC–Au complex **7** were synthesized according to Scheme 3. In the ^1H NMR spectrum of **6**, a low-field resonance at 12.03 ppm was attributable to the C2 hydrogen atom on the imidazole. As an indication of successful metalation, the C2 proton resonance was absent in the spectrum of complex **7**. Also, in the $^{13}\text{C}\{^1\text{H}\}$ NMR spectrum of complex **7**, the carbene carbon resonance appeared at 180.5 ppm, indicative of a NHC–Au^I bond.



Scheme 3. Synthesis of the fluorescent Pfp-ester-functionalized complex **7**. TBAB = tetrabutylammonium bromide.

In analogy with the synthesis of **sgc8c-3**, complex **7** was conjugated to FITC-modified **sgc8c** (Scheme 2, bottom; FITC = fluorescein isothiocyanate). Several key data confirmed the successful bioconjugation. The FITC–**sgc8c** aptamer alone has an HPLC retention time of 16 min, whereas the retention time for complex **7** is 35 min. After the conjugation reaction, a significant peak appeared with a retention time of 24 min. The material exiting the column at 24 min was collected, dried, and analyzed. Figure 2 depicts the emission spectrum of the NHC–Au^I–FITC–**sgc8c** conjugate **sgc8c-7**. The emission maxima for the NHC fragment at 418 nm and the FITC dye at 516 nm are strong evidence for the successful conjugation reaction and formation of **sgc8c-7**. The conjugate **sgc8c-7** showed enhanced cytotoxicity ($\text{IC}_{50} = (2.39 \pm 1.50) \mu\text{M}$) as compared to that of complex **7** alone ($\text{IC}_{50} = (31.1 \pm 2.11) \mu\text{M}$) against the targeted CCRF-CEM cell line (Figure 3).

CCRF-CEM leukemia cells express the PTK-7 protein, which is recognized by the **sgc8c-7** aptamer conjugate. In contrast, K562 leukemia cells do not overexpress PTK-7, and therefore should not have any appreciable binding affinity for **sgc8c-7**. To demonstrate the selectivity of **sgc8c-7** between these cell lines, we performed a flow cytometry experiment. Figure 4 depicts the fluorescence-intensity results for K562 cells (left) and CCRF-CEM cells (right). The **sgc8c** aptamer alone was used as a positive control, and complex **7**

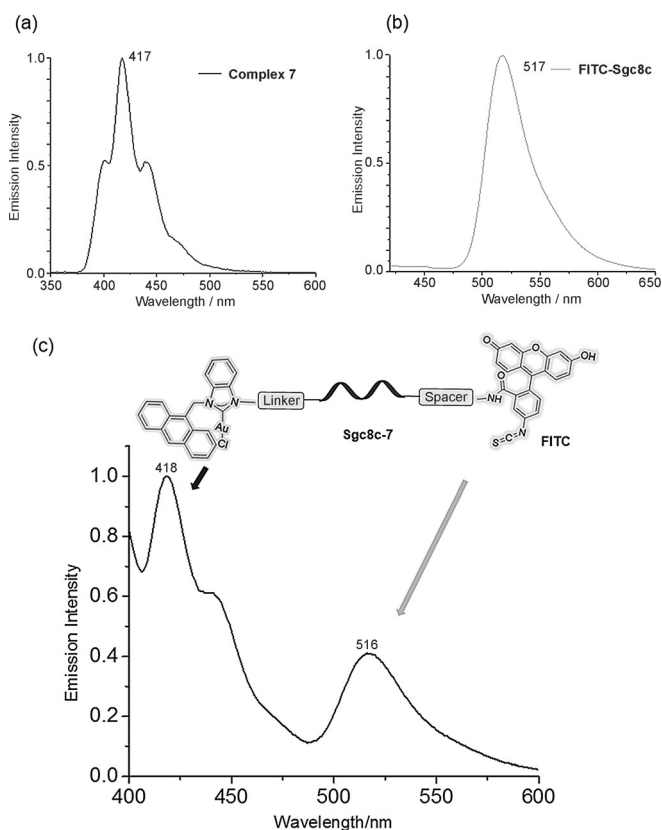


Figure 2. a) Emission spectrum of complex **7** (1:1 acetonitrile/H₂O). b) Emission spectrum of the complex FITC–**sgc8c** (1:1 acetonitrile/H₂O). c) Emission spectrum of the HPLC-separated aptamer–drug conjugate **sgc8c-7** exhibiting the emission of both the NHC–Au^I and FITC–aptamer fragments (1:1 acetonitrile/H₂O).

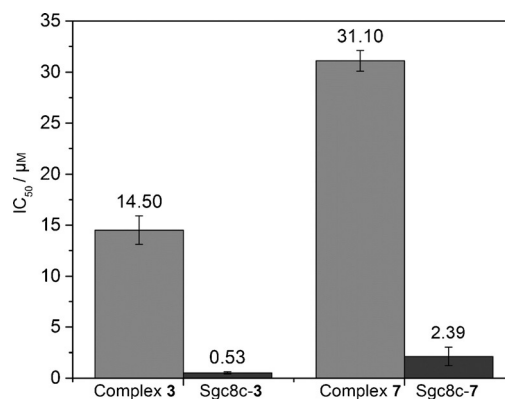


Figure 3. Comparison of the cytotoxicity of NHC–Au complexes **3** and **7** and their corresponding conjugates **sgc8c-3** and **sgc8c-7**.

conjugated to a library of random sequences tagged with FITC (**LIB-7**) was used as negative control. The enhancement of the fluorescence intensity indicates that **sgc8c-7** has a specific binding affinity for the CCRF-CEM target cells (Figure 4, right), whereas in the case of K562 cells (left), neither **LIB-7** nor **sgc8c-7** caused any clear fluorescence-intensity change.

Besides specific recognition, a drug-delivery agent should be able to be internalized into cancer cells. The aptamer **sgc8c**

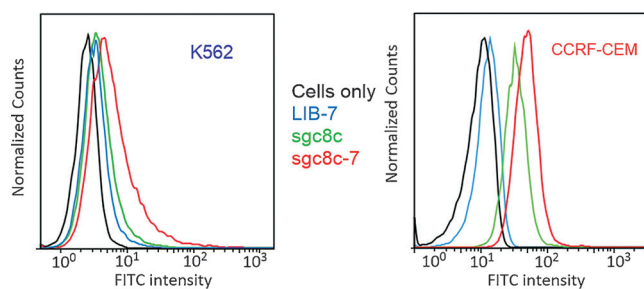


Figure 4. Flow cytometry assays of the conjugate **sgc8c-7** with the K562 cell line (left) and the CCRF-CEM cell line (right). Random aptamer sequences conjugated to **7** to create **LIB-7** were used as a negative control and did not exhibit any fluorescence-intensity change. The aptamer **sgc8c** and the conjugate **sgc8c-7**, which can target CCRF-CEM cells, exhibited fluorescence-intensity increases (see the Supporting Information for more information).

was previously reported to be internalized into target CCRF-CEM leukemia cells selectively.^[27] In our current study, **sgc8c-7** and **LIB-7** were incubated with CCRF-CEM cells and K562 cells for 4 h. Strong green fluorescence was observed from the cytoplasm of CEM cells treated with **sgc8c-7** (Figure 5a). In contrast, CEM cells treated with **LIB-7**, and K562 cells treated with **sgc8c-7** and **LIB-7** displayed negligible fluorescence, thus demonstrating the specificity of **sgc8c-7** recognition and internalization into targeted CCRF-CEM cancer cells.

Following the validation of **sgc8c-7** for selective cancer-cell recognition and internalization, we studied its selective cytotoxicity. The target CCRF-CEM cells and off-target K562 cells were incubated with **sgc8c-7** or **LIB-7** for 4 h to allow

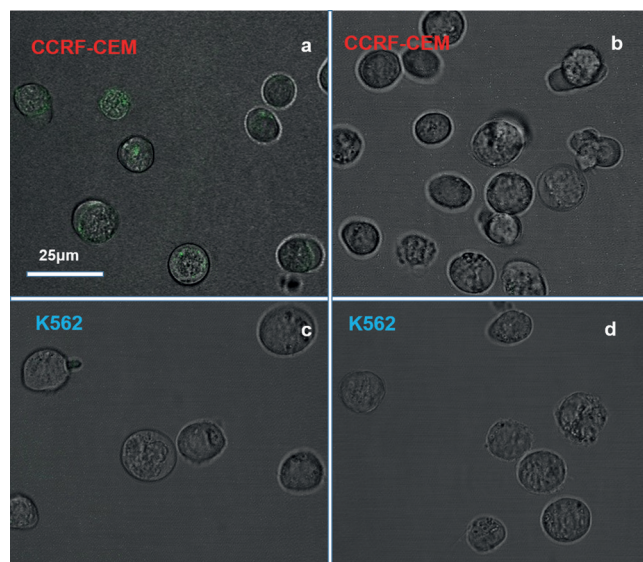


Figure 5. Confocal microscopy images of a) CEM cells incubated with **Sgc8c-7**, b) CEM cells incubated with **LIB-7**, c) K562 cells incubated with **Sgc8c-7**, and d) K562 cells incubated with **LIB-7** for 4 h at 37 °C. The **sgc8c**-aptamer and **LIB** sequences were labeled with fluorescein. Scale bars correspond to 25 μm. Only the cells treated with **Sgc8c-7** exhibited appreciable internalization, as shown by the green color in (a).

time for specific binding and internalization, then new medium was added, and the cells were incubated for another 48 h. We evaluated their cell-proliferation ability in an MTS assay. In the case of K562 cells, **sgc8c-7** did not induce appreciable cytotoxicity. However, for the target CCRF-CEM cells, **sgc8c-7** exhibited dose-dependent cytotoxicity with $IC_{50} = (2.39 \pm 1.50) \mu M$ (Figure 6). **LIB-7** was not toxic to either CEM or K562 cells. This result confirmed that we had been successful in combining the cytotoxicity of an NHC–Au complex with selectivity mediated by the **sgc8c** aptamer.

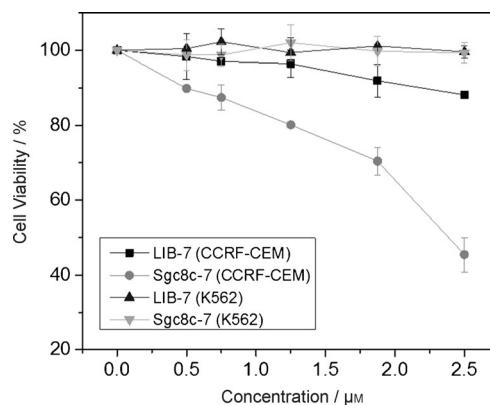


Figure 6. Results of MTS cell-proliferation assays demonstrating the specific cytotoxicity of **sgc8c-7** towards CCRF-CEM cells.

In summary, two NHC–Au^I complexes were conjugated to the CCRF-CEM-specific aptamer **sgc8c**. Fluorescent dyes tagged to the NHC–Au^I and aptamer fragments provided conclusive evidence of successful conjugation. Notably, the cytotoxicity of the NHC–Au^I ion was enhanced upon conjugation to the aptamer by a factor as high as 30. Furthermore, flow cytometry and confocal microscopy confirmed that **sgc8c-7** was able to selectively recognize and be internalized into target cancer cells. In vitro MTS cell-proliferation assays showed that **sgc8c-7** was relatively non-toxic to off-target K562 cells but acutely cytotoxic to target CCRF-CEM cancer cells. A random library of aptamers conjugated with the NHC–Au^I complex was nontoxic to both K562 and CCRF-CEM cells at 2.5 μM, thus providing evidence that the **sgc8c** DNA sequence is critical to effective delivery. Finally, given the diversity of NHC–metal complexes developed over the past decade, it is conceivable that our targeted delivery system can be applied to a wide variety of metal ions with tailored NHC ligands, and therefore opens a new opportunity for future drug development.

Acknowledgements

A.S.V. and W.T. acknowledge the University of Florida for support. This research was supported in part by the National Institutes of Health (GM079359 and GM111386).

Keywords: bioconjugation · cytotoxicity · DNA aptamers · gold · N-heterocyclic carbenes

How to cite: *Angew. Chem. Int. Ed.* **2016**, 55, 8889–8893
Angew. Chem. **2016**, 128, 9035–9039

- [1] M. N. Hopkinson, C. Richter, M. Schedler, F. Glorius, *Nature* **2014**, 510, 485–496.
- [2] S. Díez-González, N. Marion, S. P. Nolan, *Chem. Rev.* **2009**, 109, 3612–3676; T. Dröge, F. Glorius, *Angew. Chem. Int. Ed.* **2010**, 49, 6940–6952; *Angew. Chem.* **2010**, 122, 7094–7107.
- [3] F. Cisnetti, A. Gautier, *Angew. Chem. Int. Ed.* **2013**, 52, 11976–11978; *Angew. Chem.* **2013**, 125, 12194–12196; W. Liu, R. Gust, *Chem. Soc. Rev.* **2013**, 42, 755–773.
- [4] M.-L. Teyssot, A.-S. Jarrousse, M. Manin, A. Chevy, S. Roche, F. Norre, C. Beaudoin, L. Morel, D. Boyer, R. Mahiou, A. Gautier, *Dalton Trans.* **2009**, 6894–6902.
- [5] B. K. Rana, A. Nandy, V. Bertolasi, C. W. Bielawski, K. Das Saha, J. Dinda, *Organometallics* **2014**, 33, 2544–2548; H. G. Raubenheimer, S. Cronje, *Chem. Soc. Rev.* **2008**, 37, 1998–2011; E. Schuh, C. Pflueger, A. Citta, A. Folda, M. P. Rigobello, A. Bindoli, A. Casini, F. Mohr, *J. Med. Chem.* **2012**, 55, 5518–5528; B. Bertrand, L. Stefan, M. Pirrotta, D. Monchaud, E. Bodio, P. Richard, P. Le Gendre, E. Warmerdam, M. H. de Jager, G. M. M. Groothuis, M. Picquet, A. Casini, *Inorg. Chem.* **2014**, 53, 2296–2303; M. E. Garner, W. Niu, X. Chen, I. Ghiviriga, K. A. Abboud, W. Tan, A. S. Veige, *Dalton Trans.* **2015**, 44, 1914–1923.
- [6] M. M. Mkandawire, M. Lakatos, A. Springer, A. Clemens, D. Appelhaus, U. Krause-Buchholz, W. Pompe, G. Roedel, M. Mkandawire, *Nanoscale* **2015**, 7, 10634–10640.
- [7] J. L. Hickey, R. A. Ruhayel, P. J. Barnard, M. V. Baker, S. J. Berners-Price, A. Filipovska, *J. Am. Chem. Soc.* **2008**, 130, 12570–12571.
- [8] E. Wong, C. M. Giandomenico, *Chem. Rev.* **1999**, 99, 2451–2466; C. A. Rabik, M. E. Dolan, *Cancer Treat. Rev.* **2007**, 33, 9–23; C. Monneret, *Ann. Pharm. Fr.* **2011**, 69, 286–295.
- [9] C. K. Mirabelli, R. K. Johnson, C. M. Sung, L. Faucette, K. Muirhead, S. T. Crooke, *Cancer Res.* **1985**, 45, 32–39; C. K. Mirabelli, R. K. Johnson, D. T. Hill, L. F. Faucette, G. R. Girard, G. Y. Kuo, C. M. Sung, S. T. Crooke, *J. Med. Chem.* **1986**, 29, 218–223.
- [10] D. Chen, V. Milacic, M. Frezza, Q. P. Dou, *Curr. Pharm. Des.* **2009**, 15, 777–791.
- [11] A. D. Ellington, J. W. Szostak, *Nature* **1990**, 346, 818–822; D. Shangguan, Y. Li, Z. Tang, Z. C. Cao, H. W. Chen, P. Mallikaratchy, K. Sefah, C. J. Yang, W. Tan, *Proc. Natl. Acad. Sci. USA* **2006**, 103, 11838–11843.
- [12] H. Ma, J. Liu, M. M. Ali, M. A. I. Mahmood, L. Labanieh, M. Lu, S. M. Iqbal, Q. Zhang, W. Zhao, Y. Wan, *Chem. Soc. Rev.* **2015**, 44, 1240–1256; S. S. Oh, B. F. Lee, F. A. Leibfarth, M. Eisenstein, M. J. Robb, N. A. Lynd, C. J. Hawker, H. T. Soh, J. Am. Chem. Soc. **2014**, 136, 15010–15015; Y.-A. Shieh, S.-J. Yang, M.-F. Wei, M.-J. Shieh, *ACS Nano* **2010**, 4, 1433–1442; S. Dhar, F. X. Gu, R. Langer, O. C. Farokhzad, S. J. Lippard, *Proc. Natl. Acad. Sci. USA* **2008**, 105, 17356–17361.
- [13] D. Kim, Y. Y. Jeong, S. Jon, *ACS Nano* **2010**, 4, 3689–3696; V. Bagalkot, O. C. Farokhzad, R. Langer, S. Jon, *Angew. Chem. Int. Ed.* **2006**, 45, 8149–8152; *Angew. Chem.* **2006**, 118, 8329–8332.
- [14] Y.-F. Huang, D. Shangguan, H. Liu, J. A. Phillips, X. Zhang, Y. Chen, W. Tan, *ChemBioChem* **2009**, 10, 862–868.
- [15] R. Wang, G. Zhu, L. Mei, Y. Xie, H. Ma, M. Ye, F.-L. Qing, W. Tan, *J. Am. Chem. Soc.* **2014**, 136, 2731–2734.
- [16] L. A. Ahmed, S. A. El-Maraghy, *Biochem. Pharmacol.* **2014**, 92, 517–517.
- [17] B. C. Pestalozzi, G. A. Sotos, P. L. Choyke, J. S. Fisherman, K. H. Cowan, J. A. Oshaughnessy, *Cancer* **1993**, 71, 1797–1800.
- [18] L. Smith, M. B. Watson, S. L. O’Kane, P. J. Drew, M. J. Lind, L. Cawkwell, *Mol. Cancer Ther.* **2006**, 5, 2115–2120.
- [19] X. Fang, W. Tan, *Acc. Chem. Res.* **2010**, 43, 48–57.
- [20] A. Radzicka, R. Wolfenden, *J. Am. Chem. Soc.* **1996**, 118, 6105–6109.
- [21] J. Kalia, R. T. Raines, *Curr. Org. Chem.* **2010**, 14, 138–147.
- [22] C. Montalbetti, V. Falque, *Tetrahedron* **2005**, 61, 10827–10852; J. M. Humphrey, A. R. Chamberlin, *Chem. Rev.* **1997**, 97, 2243–2266.
- [23] J. Lemke, N. Metzler-Nolte, *Eur. J. Inorg. Chem.* **2008**, 3359–3366.
- [24] T. Chen, M. I. Shukoor, R. Wang, Z. Zhao, Q. Yuan, S. Bamrungsap, X. Xiong, W. Tan, *ACS Nano* **2011**, 5, 7866–7873.
- [25] A. D. Keefe, S. Pai, A. Ellington, *Nat. Rev. Drug Discovery* **2010**, 9, 537–550.
- [26] J. Zhou, J. J. Rossi, *Mol. Ther. Nucleic Acids* **2014**, 3, e169.
- [27] Z. Xiao, D. Shangguan, Z. Cao, X. Fang, W. Tan, *Chem. Eur. J.* **2008**, 14, 1769–1775.
- [28] R. Mahato, W. Tai, K. Cheng, *Adv. Drug Delivery Rev.* **2011**, 63, 659–670.
- [29] A. Citta, E. Schuh, F. Mohr, A. Folda, M. L. Massimino, A. Bindoli, A. Casini, M. P. Rigobello, *Metallomics* **2013**, 5, 1006–1015.

Received: March 17, 2016

Published online: June 17, 2016